Published in final edited form as:
Biochemistry. 2008 October 21; 47(42): 11070–11076. doi:10.1021/bi8012406.

Using an Amino Acid Fluorescence Resonance Energy Transfer Pair To Probe Protein Unfolding: Application to the Villin Headpiece Subdomain and the LysM Domain†

Julie M. Glasscock‡, **Yongjin Zhu**§, **Pramit Chowdhury**§, **Jia Tang**§, and **Feng Gai***,§
Department of Chemistry and Department of Biochemistry and Molecular Biophysics, University of Pennsylvania, Philadelphia, Pennsylvania 19104

Abstract

Previously, we have shown that *p*-cyanophenylalanine (Phe_{CN}) and tryptophan (Trp) constitute an efficient fluorescence resonance energy transfer (FRET) pair that has several advantages over commonly used dye pairs. Here, we aim to examine the general applicability of this FRET pair in protein folding–unfolding studies by applying it to the urea-induced unfolding transitions of two small proteins, the villin headpiece subdomain (HP35) and the lysin motif (LysM) domain. Depending on whether Phe_{CN} is exposed to solvent, we are able to extract either qualitative information about the folding pathway, as demonstrated by HP35, which has been suggested to unfold in a stepwise manner, or quantitative thermodynamic and structural information, as demonstrated by LysM, which has been shown to be an ideal two-state folder. Our results show that the unfolding transition of HP35 reported by FRET occurs at a denaturant concentration lower than that measured by circular dichroism (CD) and that the loop linking helix 2 and helix 3 remains compact in the denatured state, which are consistent with the notion that HP35 unfolds in discrete steps and that its unfolded state contains residual structures. On the other hand, our FRET results on the LysM domain allow us to develop a model for extracting structural and thermodynamic parameters about its unfolding, and we find that our results are in agreement with those obtained by other methods. Given the fact that Phe_{CN} is a non-natural amino acid and, thus, amenable to incorporation into peptides and proteins via existing peptide synthesis and protein expression methods, we believe that the FRET method demonstrated here is widely applicable to protein conformational studies, especially to the study of relatively small proteins.

Fluorescence resonance energy transfer (FRET)[1] is one of the most commonly used methods for probing the distance between two sites in biological systems (1). In particular, FRET has proven to be very useful and informative in probing the conformation, conformational change, and conformational dynamics of proteins (2, 3). However, the

†Supported by the National Institutes of Health (GM-065978). J.M.G. is a trainee of the NIH Structural Biology Training Program at the University of Pennsylvania.

*To whom correspondence should be addressed. gai@sas.upenn.edu. Phone: (215) 573-6256. Fax: (215) 573-2112.
‡Department of Biochemistry and Molecular Biophysics.
§Department of Chemistry.

[1]Abbreviations: CD, circular dichroism; FRET, fluorescence resonance energy transfer; HP35; villin headpiece subdomain; LysM, lysin motif; Phe_{CN}, *p*-cyanophenylalanine.

application of FRET to protein conformational studies is not without its limitations. For example, the commonly available dye FRET pairs are bulky in comparison to amino acid side chains and, therefore, may introduce undesirable structural perturbations to the protein. For this reason, dye attachment is often restricted to solvent-exposed or relatively unstructured sites, which in turn may limit the amount of information that can be extracted from FRET. In addition, dye labeling reactions are often incomplete and/or nonspecific, leading to skewed FRET results (4). Recently, it has been shown that a nitrile-derivatized phenylalanine residue, *p*-cyanophenylalanine (Phe_{CN}), and tryptophan (Trp) constitute an efficient donor–acceptor pair for FRET measurements and were used to investigate the conformational distribution of a 14-residue peptide in aqueous solution and also the membrane-mediated helix folding kinetics of an antimicrobial peptide (5–7). Here we further demonstrate that this amino acid FRET pair can also be used to characterize, sometimes quantitatively, protein folding and unfolding transitions.

Compared to commonly used dye fluorophores, the Phe_{CN}–Trp FRET pair offers several advantages in protein conformational studies, especially for proteins that are less tolerant to structural perturbations. First, Phe_{CN} is a non-natural amino acid that can be easily incorporated into peptides through standard solid-phase peptide synthesis or into proteins using modified expression protocols (8). Second, Phe_{CN} is considered a derivative of both phenylalanine (Phe) and tyrosine (Tyr), so it only minimally perturbs the native structure, especially when used to substitute for a Phe or Tyr residue. For example, Phe_{CN} has recently been incorporated into the hydrophobic core of protein NTL9, and the resultant mutant (Phe19Phe_{CN}) exhibited folding thermodynamic properties almost identical to those of the parent protein (9). Third, the Förster distance of the Phe_{CN}–Trp pair is ~16 Å, making it well-suited for probing relatively short separation distances along a certain polypeptide sequence. Finally, the C≡N stretching vibration of Phe_{CN} is sensitive to environment (10); thus, it can also be used independently as an infrared (IR) probe (8, 10, 11). While it is expected that the Phe_{CN}–Trp FRET pair is well-suited for protein folding and unfolding studies, its general applicability has yet to be demonstrated. Herein, we apply it to study the urea-induced unfolding of two small proteins, the chicken villin headpiece subdomain, HP35 (12, 13), and the LysM domain from *Escherichia coli* membrane-bound lytic murein transglycosylase D (MltD) (14). We aim to show that this FRET pair is useful for probing distance information from within the hydrophobic core of proteins and also to extract thermodynamic information.

Because of its small size and very fast folding rate, the folding mechanism of HP35 has been extensively studied using both experimental (15–20) and computational (21–33) methods. As shown (Figure 1a), HP35 (sequence, L_{42}SDEDF-KAVF-GMTRSAFANL-PLWKQQNLKK-EKGLF$_{76}$) folds into a three-helix bundle, which is stabilized by a hydrophobic core composed of primarily three Phe residues (i.e., Phe47, Phe51, and Phe58) and Val50 (13). In addition, the single Trp residue in HP35 is conveniently located at a solvent-exposed position and is approximately 12 Å from Phe58 based on the NMR structure. The latter is well within the Förster distance of the Phe_{CN}–Trp pair, making the Phe58/Phe_{CN} mutant (hereafter called HP35-P) a good model system for monitoring the unfolding of the loop linking helix 2 and helix 3.

The LysM domain is a widespread protein module originally identified in enzymes that degrade bacterial cell walls and is primarily associated with peptidoglycan binding (34). As shown (Figure 1b), the LysM domain of MltD folds into a $\beta\alpha\alpha\beta$ motif in which the two helices pack onto the same side of a two-stranded antiparallel β-sheet. In addition, it contains a single Trp residue (sequence, SITYRVRKG-DSLSSIAKRH-GVNIKDVMRW-NSDTANLQPG-DKLTLFVK), thus making it convenient to employ the proposed FRET study. More importantly, Nickson et al. (35) have recently used extensive Φ-value analyses to show that LysM is an ideal two-state folder and the ΔG for unfolding at 10 °C is 3.0 kcal/mol. To conduct the proposed FRET study, we replaced the C-terminal Lys residue with Phe_{CN} and the resultant mutant is called LysM-P hereafter.

In both cases, our results show that the global unfolding transitions can be followed by Phe_{CN}–Trp FRET. However, depending on the protein in question and also on the locations of the donor and acceptor, this FRET pair can reveal subtle details that may be obscured in measurements employing other conformational probes. Thus, this study demonstrates the utility of the Phe_{CN}–Trp FRET pair as a versatile conformational marker in protein folding studies.

MATERIALS AND METHODS

Materials

HP35-P and LysM-P were synthesized on a peptide synthesizer (Protein Technologies) using Rink resin. Peptides were then purified to homogeneity by reverse-phase HPLC. The identity of the peptide was further verified by matrix-assisted laser desorption ionization mass spectrometry.

CD Measurements

The far-UV circular dichroism (CD) spectra of HP35-P were measured on a 62A DS spectropolarometer (Aviv Associates) with a 1 mm sample cell. The HP35-P concentration was 23.9 μM as determined by its absorbance at 280 nm.

Absorption Measurement

All UV–vis spectra were measured on a Lambda 25 UV–vis spectrometer (Perkin-Elmer). The Fourier transform infrared (FTIR) spectrum of HP35-P in the C≡N stretching region was recorded at 26 °C on a Magna-IR 860 spectrometer (Nicolet) at 2 cm^{-1} resolution using a two-compartment CaF_2 sample cell.

Fluorescence Measurements

The fluorescence spectra at 2 nm resolution were obtained on a Fluorolog 3.10 spectrofluorometer (Jobin Yvon Horiba) using a 1 cm quartz sample cell. All LysM-P urea titrations were conducted at 20 °C and in 20 mM phosphate buffer (pH 5.8), and the peptide concentration was 10 μM. Similarly, all HP35-P urea titrations were conducted at 20 °C and in 50 mM phosphate buffer (pH 7), and the peptide concentration was 7 μM. Temperature was regulated using a TLC 50 Peltier temperature controller (Quantum Northwest). To minimize self-quenching, the optical density (OD) of each sample at the excitation

wavelength was adjusted to be in the range of 0.1–0.2. To achieve a high signal-to-noise (S/N) ratio, an integration time of 2 s/nm was used in HP35-P experiments and 1.5 s/nm for the LysM-P experiments. Although the relatively long integration time could result in sample photobleaching, control experiments showed that the emission intensity changed less than 5% during an hour of measurement, demonstrating that the effect of photobleaching was minimal in these measurements.

RESULTS AND DISCUSSION

As an amino acid FRET pair, the Phe_{CN}–Trp pair is expected to offer distinct advantages over commonly used dye fluorophores, especially in studies involving conformational changes of peptides and/or small proteins or conformational events occurring over a relatively short distance. For example, this FRET pair has recently been used to reveal the conformational distribution of short unstructured peptides in solution (5). Here we use two small proteins, HP35 and the LysM domain, to show that the Phe_{CN}–Trp FRET pair not only is broadly applicable to protein folding–unfolding studies but also can reveal either local or global folding–unfolding transitions, depending on the locations of the donor and acceptor and also the protein in question.

Application to HP35

HP35 provides an attractive model system for testing the utility of the Phe_{CN}–Trp FRET pair in protein folding–unfolding studies because it conveniently consists of a single Trp residue and three Phe residues that are structurally important and also tolerable to mutation (36). Here, we have chosen to mutate Phe58 to Phe_{CN} based on earlier studies that suggested it to be one of the most critical residues for defining the native fold of this protein (31, 33). Moreover, Phe58 and Trp64 are located on two helices that are separated by a short loop. Thus, this mutation might also prove to be useful in providing information about the conformational flexibility of the aforementioned loop, the formation of which has been suggested to be an important step in villin headpiece folding (33, 37, 38).

As shown (Figure 2), the CD spectrum of HP35-P shows characteristics of helical proteins, indicating that the mutation does not lead to significant disruption of the fold. In addition, the fluorescence spectrum of HP35-P in buffer, obtained by using an excitation wavelength of 240 nm where the absorbance of Trp is much smaller than that of Phe_{CN} (5), exhibits the characteristics of FRET (Figure 3). In particular, the donor fluorescence is quenched almost completely, indicating that the distance between the donor and acceptor is well within the Förster distance of the FRET pair. This is in agreement with the fact that in the folded state of HP35, the distance from Phe58 to Trp64 (Cα to Cα) is only 12 Å, significantly shorter than the R_0 of the Phe_{CN}–Trp FRET pair (~16 Å). As expected (Figure 3), addition of urea causes the Phe_{CN} fluorescence to increase, indicating that the separation distance between the donor and acceptor increases as a result of urea-induced protein unfolding. Interestingly, however, the Trp fluorescence also shows a concomitant increase, indicative of deviation from a simple scenario in which the FRET signal is a function of only the donor–acceptor distance (see below).

To provide a more quantitative assessment of the acquired FRET data, we decomposed the measured fluorescence spectra into their constituent spectral components, i.e., the fluorescence spectra of the donor and acceptor. This was accomplished by fitting an individual spectrum (i.e., the spectrum obtained at a certain urea concentration), $F_{obs}(\lambda)$, to the following equation:

$$F_{obs}(\lambda)=F_{DA}(\lambda)+F_{AD}(\lambda) \quad (1)$$

where $F_{DA}(\lambda)$ represents the fluorescence spectrum of the donor in the presence of the acceptor and is calculated as $\alpha I(\lambda)$, where $I(\lambda)$ is the emission spectrum of free Phe_{CN} measured under the same experimental conditions and α is a constant which was allowed to vary during the fitting process. In addition, $F_{AD}(\lambda)$, the fluorescence spectrum of the acceptor in the presence of the donor, was modeled by two Gaussian functions whose amplitude, position, and width were allowed to vary in the fit. As shown (Figure 4a), the integrated areas of the emission spectra of Phe_{CN} and Trp increase with an increase in urea concentration, suggesting that either the quantum yield of the donor, that of the acceptor, or both are changing upon denaturation. Indeed, the Trp fluorescence of HP35-P, measured using an excitation wavelength of 290 nm where the absorbance of Trp overwhelms that of Phe_{CN}, shows a monotonic increase as a function of urea concentration (data not shown). In addition, it has been shown that the quantum yield of Phe_{CN} is environment-dependent, with a lower quantum yield in a more hydrophobic environment (9, 39). Thus, in the case presented here, the quantum yield of Phe_{CN} is expected to increase upon protein unfolding as it becomes more hydrated in the denatured state. Indeed, the C≡N stretching vibration of HP35-P in its folded state is centered around 2235 cm^{-1} (Figure 2, inset), indicating that the Phe_{CN} residue is only partially exposed to solvent (10).

These factors make it difficult to extract any quantitative information (e.g., distance) from the corresponding FRET measurements. However, the ratio of donor to acceptor fluorescence intensity (hereafter termed R_{DA}) at each urea concentration reports an apparent FRET efficiency which is determined by several factors, including the donor-to-acceptor distance, the Förster distance, which changes as a function of urea concentration, and the quantum yield of the acceptor (Trp). Despite potential complications arising from these factors, such a plot is advantageous in that it eliminates the need for a reference protein in which the acceptor is absent and intrinsically corrects for the uncertainty arising from variation in protein concentration and excitation energy at each urea concentration. As shown (Figure 4b), the R_{DA} of HP35-P exhibits a monotonic increase with an increase in urea concentration and reaches a plateau at ~5 M urea, indicating that once unfolded the distance between Phe_{CN} and Trp in HP35-P is not sensitive to a further increase in the concentration of the denaturant. The FRET efficiency (E) can be determined from the ratio of F_{DA}/F_D, where F_D is the donor fluorescence intensity when the acceptor is absent. At 7.5 M urea, the C≡N stretching frequencies of HP35-P and free Phe_{CN} are within 1 cm^{-1} of each other (data not shown), suggesting that the Phe_{CN} side chain in the unfolded protein is largely exposed to solvent. Thus, we have estimated E and consequently the separation distance between the donor and acceptor in the unfolded state of HP35-P using the fluorescence intensity of free Phe_{CN}. Assuming that the quantum yield of free Phe_{CN} is similar to that of Phe_{CN} in the unfolded HP35-P without the presence of Trp, the ensemble-

averaged separation distance between Phe_{CN} and Trp at 8 M urea is estimated to be ~13.1 ± 2.0 Å, which indicates that the loop sandwiched between Phe_{CN} and Trp is rigid and also suggests that the unfolded state of HP35 is rather compact. The latter is consistent with the notion that a significant amount of residual structure exists in the denatured state of the villin headpiece (18, 40) and also the simulation studies of Duan and co-workers (33, 37), which concluded that this loop plays an important role in initiating the folding of HP35 by locking down the movements of helices harboring the FRET pair. Thus, the rigidity of this loop may contribute to the ultrafast folding rate of HP35 (16, 17) as it has been shown that loop formation plays an important role in controlling the folding kinetics of helix–turn–helix motifs (41). In support of this, NMR and CD experiments have shown that one highly conserved residue in the turn (42) is critical for folding (38).

Interestingly, the urea-induced unfolding transition reported by FRET (i.e., R_{DA} vs [urea]) shows measurable difference from that reported by CD which monitors the total helical content of the protein (Figure 4b). Specifically, the change in FRET signal occurs at a urea concentration lower than that reported by CD. These results suggest that the two helical segments harboring the FRET pair undergo an expansion prior to the unfolding of individual helical structures. This observation is corroborated by the study of Brewer et al. (19), which showed that Ala57 becomes more solvent-exposed prior to global unfolding, and also the NMR study of Tycko and co-workers (43), which indicates a higher secondary structure content in protein molecules with disrupted tertiary structure. Finally, our result is also in accord with the molecular dynamics simulation of Bandyopadhyay et al. (31), where the Phe58 residue was shown to be the nucleation site for the unfolding process of HP35.

Application to the LysM Domain

The quantum yield of Phe_{CN} in an unstructured peptide environment is not very sensitive to urea concentration (44). Thus, it is feasible to extract more quantitative folding–unfolding information using the Phe_{CN}–Trp FRET pair, provided the Phe_{CN} is placed in a solvent-exposed position. To verify the feasibility of this, we have conducted similar FRET studies on a mutant of the LysM domain, Lys48Phe_{CN} (LysM-P). We chose the LysM domain because it is an ideal two-state folder, thus making it easier to compare thermodynamic results obtained from different spectroscopic methods. In addition, the LysM domain contains a single Trp residue located at a solvent-exposed position, making the proposed FRET experiment convenient. Furthermore, the C-terminal residue Lys48 is not only solvent-exposed but also located in an unstructured region of the protein. Thus, the Lys to Phe_{CN} mutation is expected not to perturb in any significant manner the structure and stability of the LysM domain.

As shown (Figure 5), the fluorescence spectra of LysM-P at different urea concentrations, which were obtained by exciting the Phe_{CN} residue at 240 nm, show characteristics of FRET between Phe_{CN} and Trp29. Following the protocols discussed above (i.e., eq 1), we further decompose these fluorescence spectra into their constituent Phe_{CN} and Trp fluorescence spectra. As shown (Figure 6a), the fluorescence intensity (or the integrated area of the fluorescence spectrum, F_{DA} or F_{AD}) of the donor and acceptor increases and decreases, respectively, monotonically with an increasing urea concentration, indicating that unfolding

enlarges the separation distance between the donor and acceptor. As expected, the ratio of F_{DA} to F_{AD} (Figure 6b), which is related to the FRET efficiency, shows a sigmoidal dependence on denaturant concentration, typical for a cooperative or two-state folding–unfolding transition, which is in agreement with the study of Nickson et al. (35).

It is easy to show that for a two-state folding–unfolding transition, the FRET signal or the ratio of F_{DA} to F_{AD} is determined by the following equation:

$$\frac{F_{DA}}{F_{AD}}=\frac{(Q_D r^6)_f\left(R_0{}^6+r^6\right)_u+K_{eq}(Q_D r^6)_u\left(R_0{}^6+r^6\right)_f}{\left(Q_A R_0{}^6\right)_f\left(R_0{}^6+r^6\right)_u+K_{eq}\left(Q_A R_0{}^6\right)_u\left(R_0{}^6+r^6\right)_f} \quad (2)$$

where Q_D and Q_A are the quantum yields of the donor and acceptor, respectively, while subscripts f and u refer to the folded and unfolded states, respectively. In addition, r is the distance between the donor and acceptor and R_0 is the Förster distance for the FRET pair, which is defined as (45)

$$R_0{}^6=\frac{9000\ln(10)\kappa^2 J(\lambda)Q_D}{128\pi^5\eta^4 N_A} \quad (3)$$

where η is the refractive index of the medium, N_A is Avogadro's number, κ is the orientation factor, and $J(\lambda)$ represents the overlap integral of the donor emission and the acceptor absorption profiles. Furthermore, K_{eq} is the equilibrium constant for unfolding, which is defined as

$$K_{eq}=\exp\left(\frac{-\Delta G^\circ}{RT}\right) \quad (4)$$

with

$$\Delta G^\circ=\Delta G^\circ(0)-m[\text{urea}] \quad (5)$$

where $\Delta G°(0)$ is the free energy change for unfolding in water and m is a constant (46, 47).

Equation 2 indicates that to determine K_{eq}, one needs to know both Q_D and Q_A. However, if we assume that Q_D does not change (or R_0 is a constant) upon unfolding of the LysM domain, which is valid in the current case because the Phe_{CN} is located in a solvent-exposed position, eq 2 can be simplified to

$$\frac{F_{DA}}{F_{AD}}=\left[\frac{128\pi^5 N_A\eta^4}{9000\ln(10)\kappa^2 J(\lambda)}\right]\left[\frac{r_f^6\left(R_0{}^6+r^6\right)_u+K_{eq}r_u^6\left(R_0{}^6+r^6\right)_f}{(Q_A)_f\left(R_0{}^6+r^6\right)_u+K_{eq}(Q_A)_u\left(R_0{}^6+r^6\right)_f}\right] \quad (6)$$

This equation indicates that it is possible to determine K_{eq} and r from the FRET signals if independent measurements can provide information about how the quantum yield of the

acceptor changes as a function of urea concentration. Fortunately, this can be done easily in the current case because even when Phe_{CN} is present, the Trp (acceptor) fluorescence can be selectively excited by using an excitation wavelength of 290 nm. As shown (Figure 6b), the Trp fluorescence of LysM-P obtained by directly exciting the Trp fluorophore is different from that obtained via FRET excitation. It is apparent that the unfolding transition reported by Trp fluorescence is less pronounced than that reported by FRET, due to the fact that the Trp residue in the LysM domain is largely exposed to solvent. Nonetheless, it has been used as a probe for monitoring the unfolding of this peptide (35). To determine the thermodynamics of the cooperative folding–unfolding transition of the LysM domain, we globally fit those FRET data and Trp fluorescence intensities, presented in Figure 6b, to eq 6 and the following equation:

$$\frac{F_{\mathrm{urea}}}{F_0}=\left[\frac{(Q_{\mathrm{A}})_{\mathrm{f}}+K_{\mathrm{eq}}(Q_{\mathrm{A}})_{\mathrm{u}}}{1+K_{\mathrm{eq}}}\right]_{\mathrm{urea}}\Big/\left[\frac{(Q_{\mathrm{A}})_{\mathrm{f}}+K_{\mathrm{eq}}(Q_{\mathrm{A}})_{\mathrm{u}}}{1+K_{\mathrm{eq}}}\right]_{0} \quad (7)$$

where F_{urea} represents the fluorescence intensity of Trp obtained in urea solutions while F_0 represents that obtained in buffer solution. In addition, the donor–acceptor distance r and the quantum yield of the acceptor (Q_{A}) are assumed to be linearly dependent on the concentration of urea:

$$r_{\mathrm{u}}=r_{\mathrm{u}}^{0}+p[\mathrm{urea}] \quad (8)$$

$$Q_{\mathrm{A}}=Q_{\mathrm{A}}^{0}+q[\mathrm{urea}] \quad (9)$$

During the fitting, $\Delta G°(0)$, m, r_{f}, r_{u}^{0}, Q_{A}^{0}, p, and q are treated as global parameters. As shown (Figure 6b), the best fits yield the following thermodynamic and structural parameters: $\Delta G°(0)$ = 1.4 ± 0.1 kcal/mol, m = 0.42 ± 0.05 kcal mol^{-1} M^{-1}, and r_{f} = 13 ± 2 Å. The fact that the value of $\Delta G°(0)$ determined from the FRET method is comparable to that (1.2 ± 0.2 kcal/mol) determined from CD spectroscopy (Figure 7) validates the FRET method. In addition, this result is also consistent with the study of Nickson et al. (35), which showed that the $\Delta G°$ for the unfolding of the LysM domain is 3.0 kcal/mol at 10 °C and pH 7. Since the LysM domain is more stable at neutral pH and lower temperatures (35), under the current experimental conditions (pH 5.8 and 20 °C) the LysM domain is expected to exhibit a smaller $\Delta G°(0)$. In addition, the m value recovered from the fit, 0.42 kcal mol^{-1} M^{-1}, is also very close to that calculated from a commonly used model, 0.5 kcal mol^{-1} M^{-1} (48). Finally, the obtained r_{f} value, 13 Å, matches the expected value estimated from the NMR structure of the LysM domain. Taken together, these results indicate that the above FRET model provides a reliable estimate of the folding–unfolding thermodynamics of the LysM domain, supporting the general applicability of this approach to protein conformational studies. It should be noted, however, that the F_{AD} used in this analysis contains Trp fluorescence arising from direct excitation of the fluorophore at 240 nm (39), which ranges from 3 to 10% depending on the urea concentration. This additional contribution certainly skews the $F_{\mathrm{DA}}/F_{\mathrm{AD}}$ ratios, thus introducing errors to the resultant thermodynamic and structural parameters. To achieve a more rigorous analysis, it is desirable to subtract out

such a contribution. The latter can be done simply by using either a reference protein that does not contain the Phe_{CN} donor or the Trp fluorescence data obtained with selective excitation of Trp at 290 nm in conjunction with a scaling factor (determined by the difference in Trp absorbances at 290 and 240 nm as well as the difference in the excitation intensities at these two wavelengths).

CONCLUSIONS

We have studied the urea-induced unfolding of two small proteins, the villin headpiece subdomain and the LysM domain, using a FRET method, aiming to demonstrate the utility of the Phe_{CN}–Trp FRET pair in the study of protein folding_unfolding transitions. Our results show that this FRET pair is capable of monitoring unfolding transitions with site-specific resolution. Because Phe_{CN} can be incorporated into peptides via a standard solid-phase peptide synthesis method or into proteins via genetic manipulation, this FRET pair is expected to be generally applicable to many systems. While we present a FRET method which can be used to quantitatively analyze two-state unfolding scenarios, the Phe_{CN}–Trp FRET pair perhaps is more useful and informative in the study of non-two-state proteins or those that unfold in discrete steps. Via systematic variation of the position of the Phe_{CN} (donor) or Trp residue (acceptor), it is possible to dissect the sequence or order of the conformational events involved in the folding and unfolding of the protein in question. In addition, it is also possible to use Phe_{CN} and Trp to perform more complicated FRET experiments, such as one donor and two acceptors or two donors and one acceptor. Such experiments are particularly useful in that they allow one to probe how different segments in a protein move in response to a conformational perturbation.

References

1. Sapsford KE, Berti L, Igor L, Medintz IL. Materials for fluorescence resonance energy transfer analysis: Beyond traditional donor-acceptor combinations. Angew Chem, Int Ed. 2006; 45:4562–4588.
2. Royer CA. Probing protein folding and conformational transitions with fluorescence. Chem Rev. 2006; 106:1769–1784. [PubMed: 16683754]
3. Schuler B, Eaton WA. Protein folding studied by single-molecule FRET. Curr Opin Struct Biol. 2008; 18:16–26. [PubMed: 18221865]
4. Karolin J, Fa M, Wilczynska M, Ny T, Johansson LBA. Donor-donor energy migration for determining intramolecular distances in proteins: I. Application of a model to the latent plasminogen activator inhibitor-1 (PAV-1). Biophys J. 1998; 74:11–21. [PubMed: 9449305]
5. Tucker MJ, Oyola R, Gai F. Conformational distribution of a 14 residue peptide in solution: A fluorescence resonance energy transfer study. J Phys Chem B. 2005; 109:4788–4795. [PubMed: 16851563]
6. Tucker MJ, Tang J, Gai F. Probing the kinetics of membrane-mediated helix folding. J Phys Chem B. 2006; 110:8105–8109. [PubMed: 16610913]
7. Tang J, Signarvic RS, DeGrado WF, Gai F. Role of helix nucleation in the kinetics of binding of mastoparan X to phospholipid bilayers. Biochemistry. 2007; 46:13856–13863. [PubMed: 17994771]
8. Schultz KC, Supekova L, Ryu Y, Xie J, Perera R, Schultz PG. A genetically engineered infrared probe. J Am Chem Soc. 2006; 128:13984–13985. [PubMed: 17061854]
9. Aprilakis KN, Taskent H, Raleigh DP. Use of the novel fluorescent amino acid p-cyanophenylalanine offers a direct probe of hydrophobic core formation during the folding of the N-

terminal domain of the ribosomal protein L9 and provides evidence for two-state folding. Biochemistry. 2007; 46:12308–12313. [PubMed: 17924662]

10. Getahun Z, Huang CY, Wang T, De Leon B, DeGrado WF, Gai F. Using nitrile-derivatized amino acids as infrared probes of local environment. J Am Chem Soc. 2003; 125:405–411. [PubMed: 12517152]
11. Mukherjee S, Chowdhury P, DeGrado WF, Gai F. Site-specific hydration status of an amphipathic peptide in AOT reverse micelles. Langmuir. 2007; 23:11174–11179. [PubMed: 17910485]
12. McKnight CJ, Doering DS, Matsudaira PT, Kim PS. A thermostable 35 residue subdomain within villin headpiece. J Mol Biol. 1996; 260:126–134. [PubMed: 8764395]
13. McKnight CJ, Matsudiara PT, Kim PS. NMR structure of the 35 residue villin headpiece subdomain. Nat Struct Biol. 1997; 4:180–184. [PubMed: 9164455]
14. Bateman A, Bycroft M. The structure of the LysM domain from *E. coli* membrane-bound lytic murein transglycosylase D (MltD). J Mol Biol. 2000; 299:1113–1119. [PubMed: 10843862]
15. Hansen KC, Rock RS, Larsen RW, Chan SI. A method for photoinitiating protein folding in a nondenaturing environment. J Am Chem Soc. 2000; 122:11567–11568.
16. Kubelka J, Eaton WA, Hofrichter J. Experimental tests of villin subdomain folding simulations. J Mol Biol. 2003; 329:625–630. [PubMed: 12787664]
17. Wang M, Tang Y, Sato S, Vugmeyster L, McKnight CJ, Raleigh DP. Dynamic NMR line-shape analysis demonstrates that the villin headpiece subdomain folds in the microsecond time scale. J Am Chem Soc. 2003; 125:6032–6033. [PubMed: 12785814]
18. Brewer SH, Vu DM, Tang Y, Li Y, Franzen S, Raleigh DP, Dyer RB. Effect of modulating unfolded state structure on the folding kinetics of the villin headpiece subdomain. Proc Natl Acad Sci USA. 2005; 102:16662–16667. [PubMed: 16269546]
19. Brewer SH, Song B, Raleigh DP, Dyer RB. Residue specific resolution of protein folding dynamics using isotope-edited infrared temperature jump spectroscopy. Biochemistry. 2007; 46:3279–3285. [PubMed: 17305369]
20. Gao JM, Kelly JW. Toward quantification of protein backbone-backbone hydrogen bonding energies: An energetic analysis of an amide-to-ester mutation in an α helix within a protein. Protein Sci. 2008; 17:1096–1101. [PubMed: 18434500]
21. Duan Y, Wang L, Kollman PA. The early stage of folding of villin headpiece subdomain observed in 200 ns fully solvated molecular dynamics simulation. Proc Natl Acad Sci USA. 1998; 95:9897–9902. [PubMed: 9707572]
22. Sullivan DC, Kuntz DI. Protein folding as biased conformational diffusion. J Phys Chem B. 2002; 106:3255–3262.
23. Islam SA, Karplus M, Weaver DL. Application of the diffusion-collision model to the folding of three-helix bundle proteins. J Mol Biol. 2002; 318:199–215. [PubMed: 12054779]
24. Shen MY, Freed KF. All-atom fast protein folding simulations: The villin headpiece. Proteins. 2002; 49:439–445. [PubMed: 12402354]
25. Jang SM, Kim E, Shin S, Pak Y. Ab initio folding of helix bundle proteins using molecular dynamics simulations. J Am Chem Soc. 2003; 125:14841–14846. [PubMed: 14640661]
26. Lin CY, Hu CK, Hansmann UH. Parallel tempering simulations of HP-36. Proteins. 2003; 52:436–445. [PubMed: 12866054]
27. Ripoll DR, Vila JA, Scheraga HA. Folding of the villin headpiece subdomain from random structures. Analysis of the charge distribution as a function of pH. J Mol Biol. 2004; 339:915–925. [PubMed: 15165859]
28. Herges T, Wenzel W. Free-energy landscape of the villin headpiece in an all-tom force field. Structure. 2005; 13:661–668. [PubMed: 15837204]
29. Carr JM, Wales DJ. Global optimization and folding pathways of selected α-helical proteins. J Chem Phys. 2005; 123:234901. [PubMed: 16392943]
30. Ensign DL, Kasson PM, Pande VS. Heterogeneity even at the speed limit of folding: Large-scale molecular dynamics study of a fast-folding variant of the villin headpiece. J Mol Biol. 2006; 374:806–816. [PubMed: 17950314]

31. Bandyopadhyay S, Chakraborty S, Bagchi B. Coupling between hydration layer dynamics and unfolding kinetics of HP-36. J Chem Phys. 2006; 125:084912. [PubMed: 16965062]
32. Wickstrom L, Okur A, Song K, Hornak V, Raleigh DP, Simmerling CL. The unfolded state of the villin headpiece helical subdomain: Computational studies of the role of locally stabilized structure. J Mol Biol. 2006; 360:1094–1107. [PubMed: 16797585]
33. Lei H, Duan Y. Two-stage folding of HP-35 from Ab initio simulations. J Mol Biol. 2007; 370:196–206. [PubMed: 17512537]
34. Buist G, Steen A, Kok J, Kuipers OP. LysM, a widely distributed protein motif for binding to (peptido)glycans. Mol Microbiol. 2008; 68:838–847. [PubMed: 18430080]
35. Nickson AA, Stoll KE, Clark J. Folding of a LysM domain: Entropy-enthalpy compensation in the transition state of an ideal two-state folder. J Mol Biol. 2008; 380:557–569. [PubMed: 18538343]
36. Frank BS, Vardar D, Buckley DA, McKnight CJ. The role of aromatic residues in the hydrophobic core of the villin headpiece subdomain. Protein Sci. 2002; 11:680–687. [PubMed: 11847290]
37. Lei H, Wu C, Liu H, Duan Y. Folding free-energy landscape of villin headpiece subdomain from molecular dynamics simulations. Proc Natl Acad Sci USA. 2007; 104:4925–4930. [PubMed: 17360390]
38. Vermeulen W, Van Troys M, Bourry D, Dewitte D, Rossenu S, Goethals M, Borremans FAM, Vanderkerckhove J, Martins JC, Ampe C. Identification of the PXW sequence as a structural gatekeeper of the headpiece C-terminal subdomain fold. J Mol Biol. 2006; 359:1277–1292. [PubMed: 16697408]
39. Tucker MJ, Oyola R, Gai F. A novel fluorescent probe for protein binding and folding studies: p-Cyano-phenylalanine. Biopolymers. 2006; 83:571–576. [PubMed: 16917881]
40. Tang Y, Rigotti DJ, Fairman R, Raleigh DP. Peptide models provide evidence for significant structure in the denatured state of a rapidly folding protein: The villin headpiece subdomain. Biochemistry. 2004; 43:3264–3272. [PubMed: 15023077]
41. Du D, Gai F. Understanding the folding mechanism of an α-helical hairpin. Biochemistry. 2006; 45:13131–13139. [PubMed: 17073435]
42. Vermeulen W, Vanhaesebrouck P, Van Troys M, Verschueren M, Fant F, Goethals M, Ampe C, Martins JC, Borremans FAM. Solution structures of the C-terminal headpeice subdomains of human villin and advillin, evaluation of headpiece F-actin-binding requirements. Protein Sci. 2004; 13:1276–1287. [PubMed: 15096633]
43. Havlin RH, Tycko R. Probing site-specific conformational distributions in protein folding with solid-state NMR. Proc Natl Acad Sci USA. 2005; 102:3284–3289. [PubMed: 15718283]
44. Du D, Tucker MJ, Gai F. Understanding the mechanism of β-hairpin folding via φ-value analysis. Biochemistry. 2006; 45:2668–2678. [PubMed: 16489760]
45. Förster T. Ann Phys. 1948; 2:55–75.Förster, T. Biological Physics. Mielczarek, EV.; Greenbaum, E.; Knox, RS., editors. American Institute of Physics; New York: 1993. p. 148-160.(English translation)
46. Greene RF Jr, Pace CN. Urea and guanidine hydrochloride denaturation of ribonuclease, lysozyme, α-chymotrytsin, and β-lactoglobulin. J Biol Chem. 1974; 249:5388–5393. [PubMed: 4416801]
47. Santoro MM, Bolen DW. A test of the linear extrapolation of unfolding free energy changes over an extended denaturant concentration range. Biochemistry. 1992; 31:4901–4907. [PubMed: 1591250]
48. Myers JK, Pace N, Scholtz JM. Denaturant m values and heat capacity changes: Relation to changes in accessible surface areas of protein unfolding. Protein Sci. 1995; 4:2138–2148. [PubMed: 8535251]

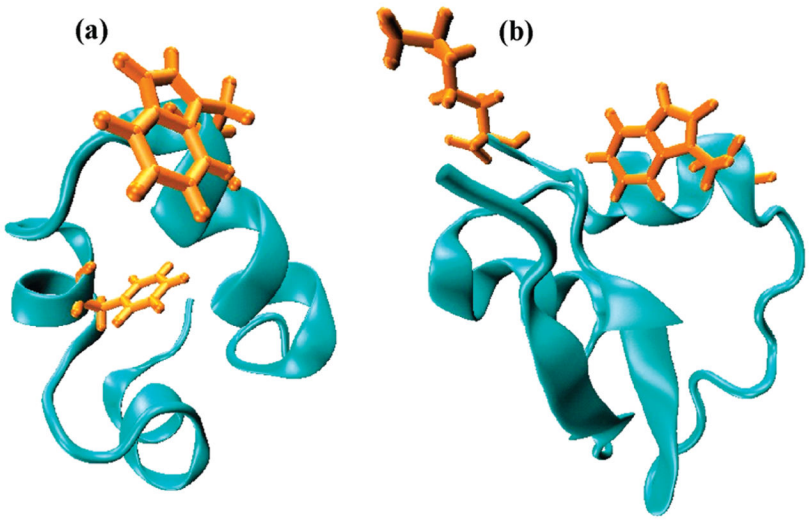

Figure 1.

(a) NMR structure of HP35 (PDB entry 1VII). (b) NMR structure of the LysM domain (PDB entry 1E0G). In both cases, the Trp side chain and the side chain of the residue which was replaced with Phe_{CN} in this study are shown.

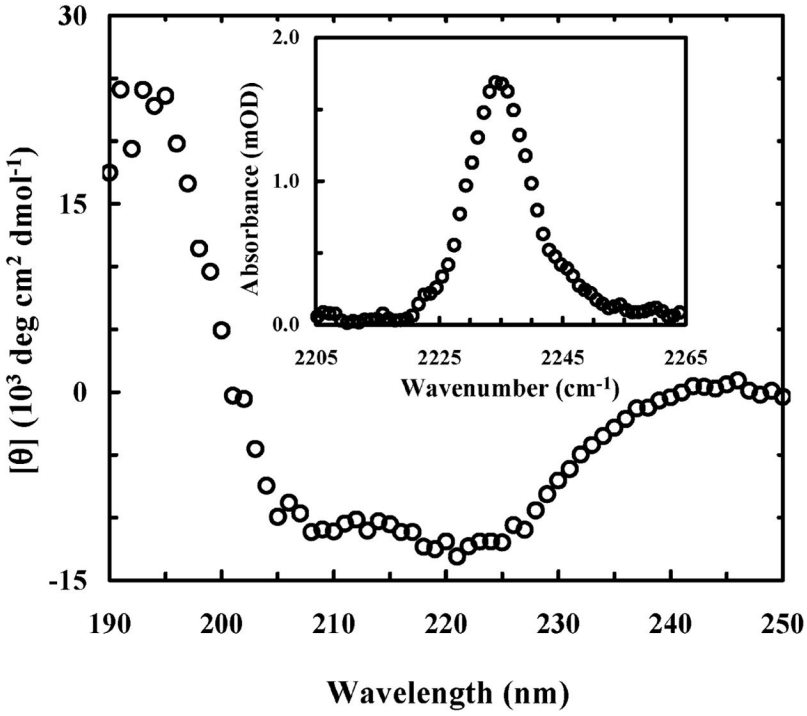

Figure 2.

CD spectrum of HP35-P collected at 25 °C. The peptide concentration was 24 μM [in 50 mM phosphate buffe (pH 7)]. The inset shows the C≡N stretching vibration of HP35-P at 26 °C.

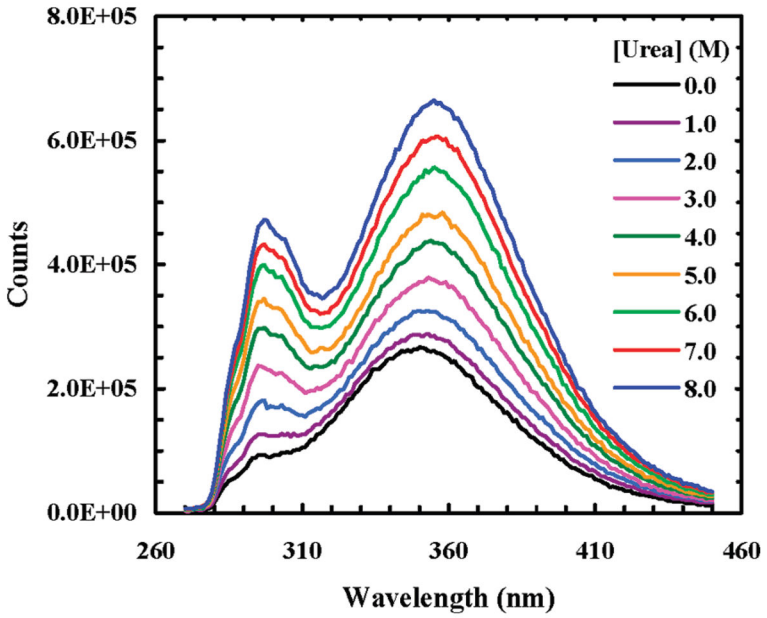

Figure 3.

Fluorescence spectra of HP35-P at different urea concentrations, as indicated in the figure. λ_{ex} = 240 nm.

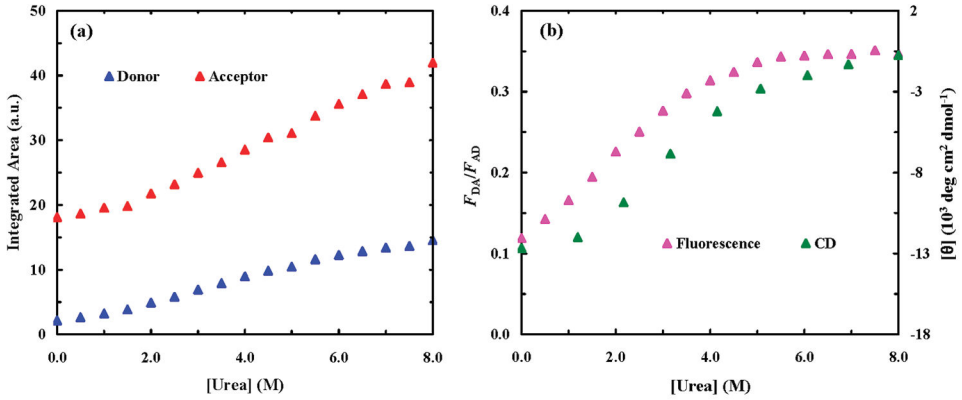

Figure 4.

(a) Fluorescence intensities (integrated area) of Phe_{CN} (blue) and Trp (red) of HP35-P as a function of urea concentration. (b) Ratio of the Phe_{CN} fluorescence intensity (F_{DA}) to the Trp fluorescence intensity (F_{AD}) vs urea concentration. Also shown is the mean residue ellipticity of HP35-P at 222 nm as a function of urea concentration.

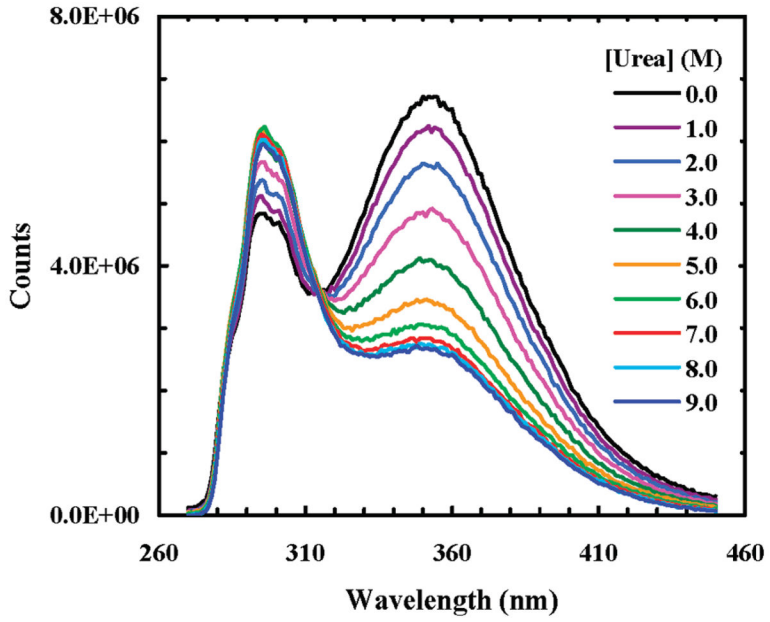

Figure 5.

Fluorescence spectra of LysM-P at different urea concentrations, as indicated in the figure. λ_{ex} = 240 nm.

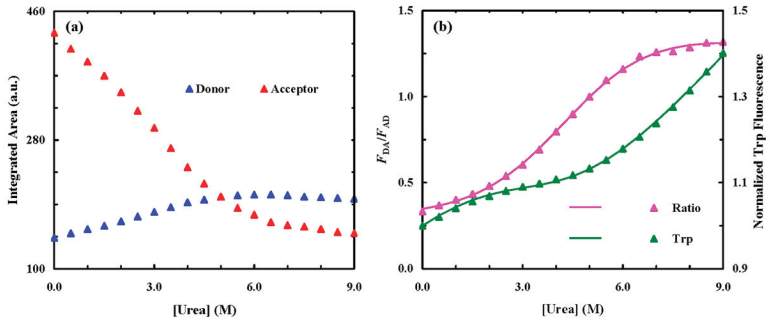

Figure 6.

(a) Fluorescence intensity (integrated area) of Phe_{CN} (blue) and Trp (red) of LysM-P as a function of urea concentration. (b) Ratio of the Phe_{CN} fluorescence intensity (F_{DA}) to the Trp fluorescence intensity (F_{AD}) vs urea concentration. Also shown is the normalized fluorescence intensity of Trp, measured upon direct excitation at 290 nm, as a function of urea concentration. Smooth lines are global fits to these data according to the methods discussed in the text.

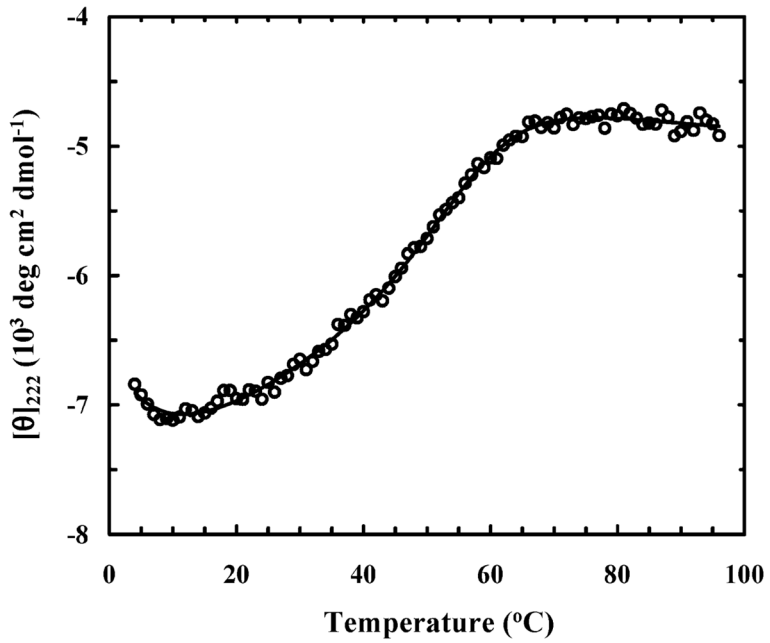

Figure 7.

Mean residue ellipticity of LysM-P at 222 nm vs temperature. The solid line is the best fit of these data to a two-state model discussed in the text.